

Production cross-sections studies of residual radionuclides from proton induced nuclear reactions on ^{nat}Mo up to 40 MeV

A. A. Alharbi,* M. McCleskey, G. Tabacaru, B. Roeder, A. Banu, A. Spiridon,
E. Simmons, L. Trache, and R. E. Tribble

The productions of radioisotopes by cyclotrons play a vital role in nuclear medicine for diagnostic studies via emission tomography, viz. single photon emission computed tomography (SPECT) and positron emission tomography (PET). Since these radioisotopes are mostly neutron deficient, they cause relatively low radiation dose to the patient. The excitation function measurements of charged particle induced reactions are needed to improve and study the ideal way for medical radioisotope production. The optimization of nuclear reaction for the production of radioisotope at a cyclotron involves a selection of the projectile energy range (the energy interval between the energy incident on the thick target and the energy at the end of it) that will maximize the yield of the product and minimize that of radionuclide impurities [1].

¹In this study, the activation technique has been used to measure the excitation function of proton-induced nuclear reactions on ^{nat}Mo up to 40 MeV. The proton beam from the K500 superconducting cyclotron of the Texas A&M Cyclotron Institute was used in the SEE beam line and target chamber. Thin foils of molybdenum with natural isotopic composition (^{92}Mo 14.84%, ^{94}Mo 9.25%, ^{95}Mo 15.92%, ^{96}Mo 16.68%, ^{97}Mo 9.55%, ^{98}Mo 24.13%, ^{100}Mo 9.63%) were used as targets. A stack was made from several groups of targets (^{nat}Mo , 50 μm) and monitor foils (^{nat}Al , 125 μm and ^{nat}Cu ,

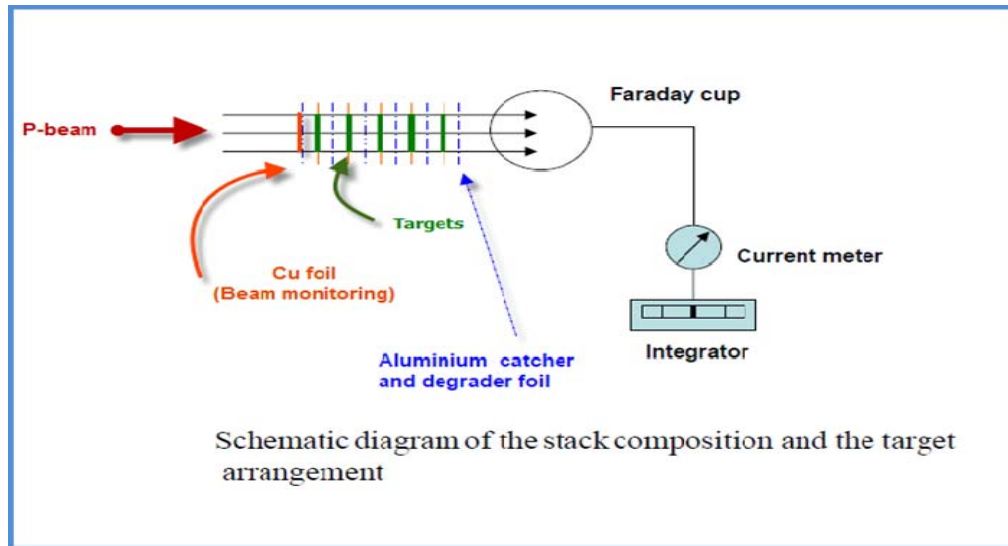


FIG. 1. Schematic diagram of the stack composition and the target arrangement.

* Fulbright Fellow 2009, On leave from Physics Department, Faculty of Sciences, Princess Nora Bint Abdul Rahman University, Riyadh, Saudi Arabia.

125 μm) that acted also as beam degraders (Fig. 1), and placed in a special aluminum target holder which was the Faraday cup to measure the beam intensity (Fig. 2). The Al and Cu monitor foils were inserted into the stack to measure the excitation functions of the well known cross-sections monitor reactions $^{27}\text{Al}(p,x)^{24}\text{Na}$ [2] and $^{\text{nat}}\text{Cu}(p,x)^{62}\text{Zn}$ [3] simultaneously with the reactions induced on the targets and were measured with the same detector and in a comparable geometry as the targets to confirm the beam intensity and energy. The stacked targets were irradiated by the 40 MeV accelerated protons at a beam current 1 nA for 65 min. The beam hits the target through an aluminum collimator of 8 mm diameter. The target foils of 10 mm diameter were sufficiently larger than the proton beam diameter (Fig. 3). Care was taken to ensure that equal areas of the monitor and the target foils intercepted the beam. The irradiation geometry used guaranteed that practically the whole beam passed through every foil.

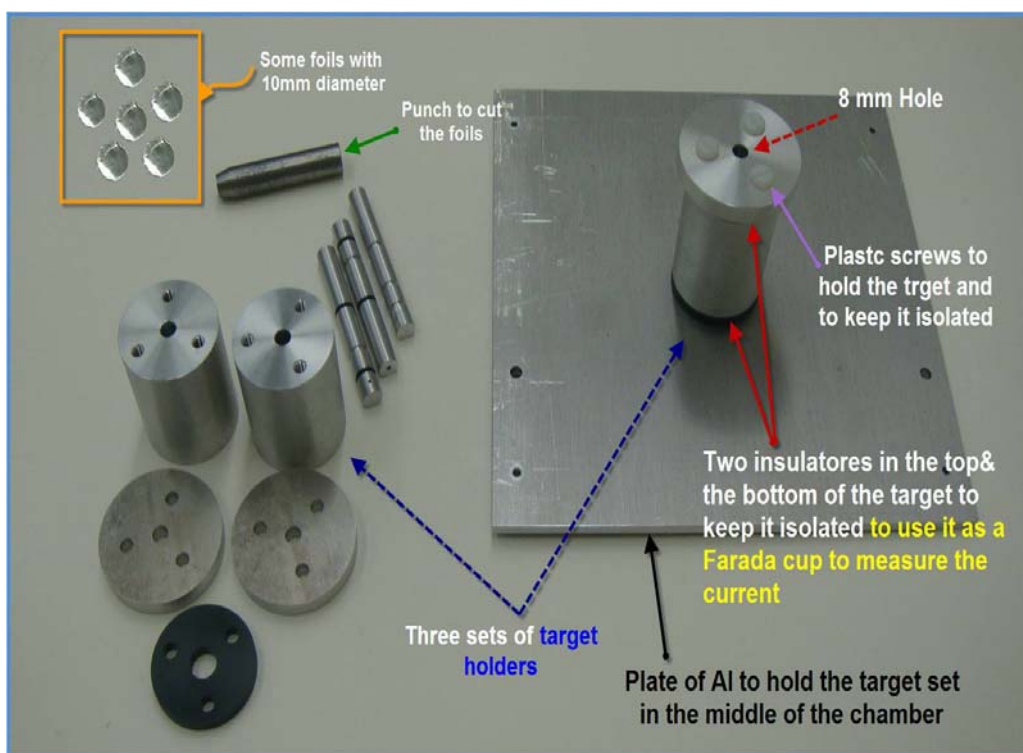


FIG. 2. A photograph for foils and the special aluminum target holders used in the experiment.

The secondary effect of the background neutrons on the molybdenum targets was checked by foils placed in the stack far behind the range of the fully stopped proton beam.

The computer program SRIM-2003 calculated the energy loss in the sample foils, as well as in the degraders [4]. The radioactivity of the residual nuclei in the activated foils was measured nondestructively using one HPGe γ -ray detector (70% relative efficiency). Each foil was recounted 2-3 times to avoid disturbance by overlapping γ -lines from undesired sources and in order to accurately evaluate cross-sections for cumulative formation of the corresponding longer-lived daughter radionuclide.

The detector-source distance was kept large enough to keep the dead time below 5% and to assure the same geometry. Several γ -lines for a nuclide will be considered to minimize the relative errors of calibration, wherever possible. Fig. 4 shows one of the measured calibrated spectrums with identified γ -lines.

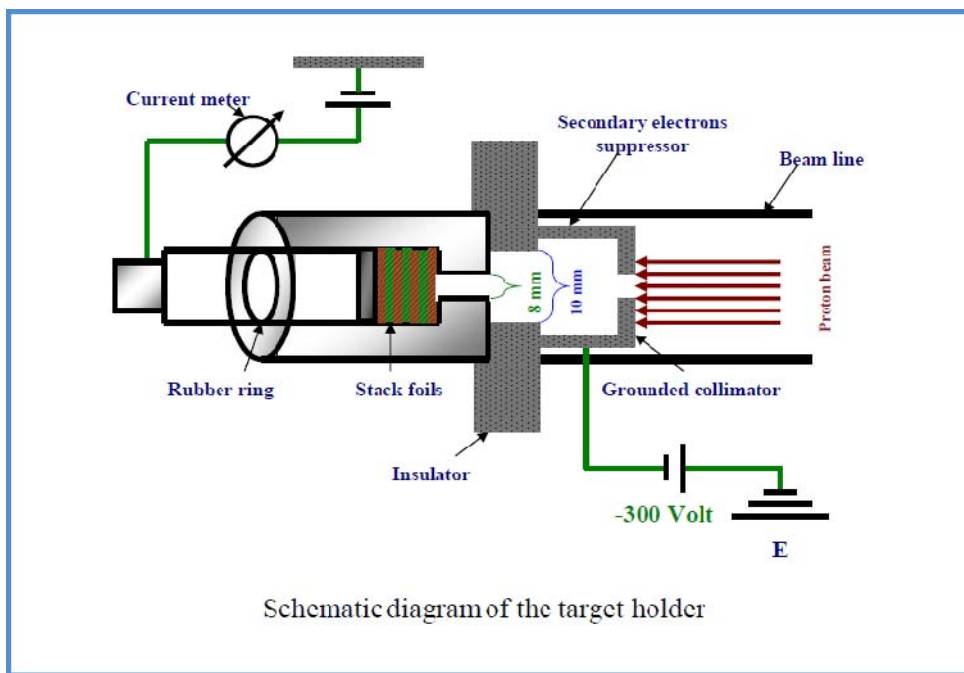


FIG. 3. Schematic diagram of the target holder setup and the faraday cup.

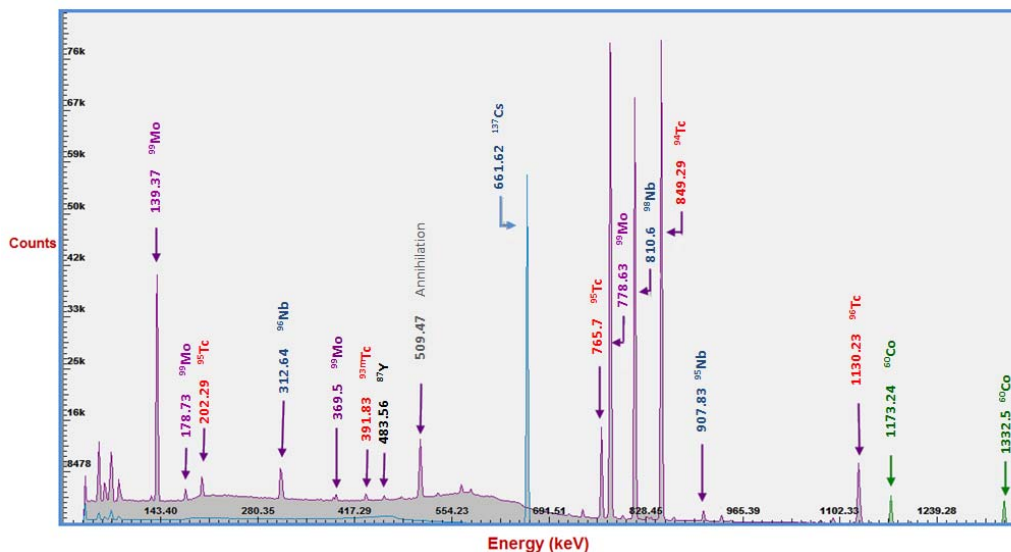


FIG. 4. A calibrated Gamma ray spectrum with identified γ -lines.

The decay data for some of the investigated radionuclides are shown in Table I. From the decay rates of the radioactive products and the measured beam current, the cross sections for the nuclear reactions $^{nat}\text{Mo}(p,X)$ will be determined using the usual activation formula. Then the determined excitation functions will be compared with the available previous published research and with the ALICE-IPPE precompound-hybrid model simulated calculations.

The integral yield of the $^{nat}\text{Mo}(p,X)$ nuclear reactions will be deduced using the excitation functions and the stopping power of ^{nat}Mo by summing the differential yield in a small energy interval (0.1 MeV) over the whole energy range [5]. It will be expressed as $\text{MBq } \mu\text{A}^{-1}\text{h}^{-1}$, i.e. for an irradiation of 1h at a beam current of 1 μA .

We will continue the program with further irradiations using 25 MeV/u alpha particles in a new location, with a chamber specially adapted for our purpose and using simultaneously two HPGe detectors for deactivation measurements.

TABLE I. Decay data of some $^{nat}\text{Mo}(p,X)$ produced radionuclides, Q-value and contributed reactions

Nuclides	Half life	Gamma-ray energy (keV)	Branching ratio (%)	Decay mode	Contributing reactions	Q-value (MeV)
^{93m}Tc	43.5 min	391.83	57.6	EC(23.3%)	$^{93}\text{Mo}(p,\gamma)$	4.08654
^{93g}Tc	2.75 h	1362.94 1520.28	66.2 24.4	EC(100%)	$^{94}\text{Mo}(p,2n)$ $^{95}\text{Mo}(p,3n)$ $^{96}\text{Mo}(p,4n)$ $^{97}\text{Mo}(p,7n)$	-13.6611 -21.0302 -30.1845 -37.0058
^{94m}Tc	52.0 min	1868.68 871.05	5.75 94.2	EC(100%) IT(0.1%)	$^{94}\text{Mo}(p,n)$ $^{95}\text{Mo}(p,2n)$ $^{96}\text{Mo}(p,3n)$ $^{97}\text{Mo}(p,4n)$ $^{98}\text{Mo}(p,5n)$	-5.0381 -12.4072 -21.5616 -28.3827 -37.0253
^{90}Mo	5.67 h	257.34 122.37	77.7 64.2	EC(100%)	$^{92}\text{Mo}(p,t)$ $^{92}\text{Mo}(p,nd)$ $^{92}\text{Mo}(p,2np)$ $^{94}\text{Mo}(p,2nt)$ $^{94}\text{Mo}(p,3nd)$ $^{95}\text{Mo}(p,3nt)$	-14.2985 -20.5558 -22.7803 -32.0461 -38.3034 -39.4152
^{89m}Nb	1.18 h	1627.2	3.4	EC(100%)	$^{92}\text{Mo}(p,\alpha)$	-1.363
^{89g}Nb	1.9 h	588	99.5	EC(100%)	$^{92}\text{Mo}(p,n^3\text{He})$ $^{92}\text{Mo}(p,2d)$ $^{92}\text{Mo}(p,2n2p)$ $^{94}\text{Mo}(p,2n\alpha)$ $^{94}\text{Mo}(p,2t)$ $^{94}\text{Mo}(p,ndt)$ $^{94}\text{Mo}(p,2npt)$ $^{95}\text{Mo}(p,3n\alpha)$ $^{95}\text{Mo}(p,n2t)$ $^{96}\text{Mo}(p,4n\alpha)$	-21.9408 -25.2097 -29.659 -19.1107 -30.4428 -36.7001 -38.9247 -26.4798 -37.8119 -35.6341

- [1] S. M. Qaim, Rad. Phys. and Chem. **71**, 917 (2004).
- [2] F. Tarkanyi *et al.*, *Beam Monitor Reactions*, IAEA-TECDOC-1211, (IAEA, Vienna, 2001) p. 49;
www-nds.iaea.or.at/medical
- [3] F. S. Al-Saleh, A. A. Al-harbi, and A. Azzam, Radiochimica Acta, **94**, 391 (2006).
- [4] J. F. Ziegler *et al.*, SRIM 2003 code, *The Stopping and Range of Ions in Solids*, (Pergamon, New York, 2003).
- [5] F. Helus and Lelio G. Colombetti, *Radionuclides Production*, (CRC Press Inc., Boca Raton, Florida, 1980).